Photoinduced Proton Transfer in a Pyridine Based Polymer Gel

Evgenia Vaganova,*,† Ellen Wachtel,‡ Gregory Leitus,‡ David Danovich,§ Stepan Lesnichin,|| Ilja G. Shenderovich,|| Hans-Henrich Limbach,|| and Shlomo Yitzchaik*,†

Institute of Chemistry and the Farkas Center for Light-Induced Processes, The Hebrew University of Jerusalem, 91904, Jerusalem, Israel, Chemical Research Support Unit, The Weizmann Institute of Science, 76100, Rehovot, Israel, Institute of Chemistry and the Lisa Meitner Center for Computational Quantum Chemistry, The Hebrew University of Jerusalem, 91904, Jerusalem, Israel, and Department of Chemistry and Biochemistry, Free University Berlin, 14195, Berlin, Germany

Received: May 11, 2010; Revised Manuscript Received: June 23, 2010

We describe an experimental and theoretical consideration of photoexcited proton transfer in a poly(4-vinyl pyridine)/pyridine gel. Evidence was found for two states of a multiple state process analyzed by DFT modeling. According to the latter, following irradiation at 385 nm, the proton donor is the CH group of the polymer main chain and the proton acceptor is the nitrogen of the polymeric pyridine side chain. Proton transfer is made possible through the assistance of a mobile pyridine solvent molecule acting as a transfer vehicle. Proton transfer promotes both a geometrical rearrangement of the vinyl side chain as well as electronic density redistribution. The photoproduct intermediate—the hydrogen-bonded complex between the protonated solvent pyridine molecule and the deprotonated polymeric pyridine side chain—is identified by its Curie law magnetic susceptibility, ESR spectrum, and fluorescence lifetime measurements. The proton transfer from the nitrogen of the solvent pyridine molecule to the pyridine side chain nitrogen, producing pyridinium, is a thermodynamically favorable relaxation process and occurs without an energy barrier. The protonation of nitrogen on the polymeric side chain was detected by solid state NMR spectroscopy performed on a ^{15}N-polymer enriched gel. The calculations and experimental data suggest a central role for the gel solvent molecule as a catalytic agent and proton transfer vehicle. The process suggested by DFT modeling may have relevance for photosensitive devices in part due to the fact that we have been able to show that long-lived paramagnetism may be included among the inducible properties of soft polymer gels.

Introduction

Soft polymer gels[1] constitute a particularly flexible state of matter in which the tuning of molecular electronic and/or geometrical properties is markedly enhanced by collective effects. Consequently, mechanical, physical, and chemical properties can be readily modified by a wide variety of factors, including electromagnetic radiation, acoustic and electric fields, temperature, composition, and pH.[2−7] Polymer gels undergoing structural changes induced by ultraviolet, visible, or near-infrared radiation have been proposed as candidates for light-sensitive memory devices, artificial muscles, and optical switches.[8−10] Currently, there is no comprehensive theory which describes the behavior of gels. Many properties are under investigation including the volume fraction of gel cross-linking points,[11] solid friction between moving segments of the polymer chain and cross-linking gel points,[12] and the concentration dependence of the polymer diffusion coefficient.[13] While intrinsic gel properties are broadly responsible for flexibility and reversibility, the particular combination of polymer, solvent, and external factors renders each system unique in its activity.

The unusual light-sensitive properties of a gel comprising the polymer poly(4-vinyl pyridine) in liquid pyridine (P4VPy/Py) have been characterized during the past few years: reversible, photoinduced conductivity which increased by as much as 50% under ultraviolet irradiation as compared to the dark state[14] and reversible changes of the ultraviolet induced emission spectrum from bright blue at 440 nm to multiple red-shifted emissions.[15] Proton transfer was suggested to play a central role in the photoinduced behavior of the poly(4-vinyl pyridine)/pyridine gel;[14] however, the mechanism could not be unambiguously identified.

Here, we present a combined experimental and theoretical investigation of the photochemical reaction. Evidence for an intermediate paramagnetic state photoproduct, an H-bonded complex between the pyridine side chain and liquid pyridine, predicted by DFT modeling, is obtained from magnetic susceptibility measurements and ESR spectroscopy. A triplet−singlet relaxation process results in the formation of protonated pyridine side chains, detected using ^{15}N NMR spectroscopy. The calculations and experimental data suggest a central role for the gel solvent molecule as a catalytic agent and proton transfer vehicle.

Experimental Methods

Materials and Methods. ***Gel Preparation.*** Poly(4-vinyl pyridine) (P4VPy, MW 50 000, Polyscience), was dried in a vacuum chamber for 1 month and then dissolved in dry pyridine (≥99.9%, Aldrich). The residual water content, according to ^{1}H NMR measurements of 0.2 mg of polymer in 0.75 mL of deuterated benzene (99.96% D), is below the sensitivity of the

* To whom correspondence should be addressed. Phone: 972 2658 6971. Fax: 972 2658 5319. E-mail: gv@cc.huji.ac.il, sy@cc.huji.ac.il.

† Institute of Chemistry and the Farkas Center for Light-Induced Processes, The Hebrew University of Jerusalem.

‡ The Weizmann Institute of Science.

§ Institute of Chemistry and the Lisa Meitner Center for Computational Quantum Chemistry, The Hebrew University of Jerusalem.

|| Free University Berlin.

10.1021/jp104277r
Published on Web 07/29/2010

SCHEME 1: Synthesis of ^{15}N-Poly(4-vinyl pyridine)

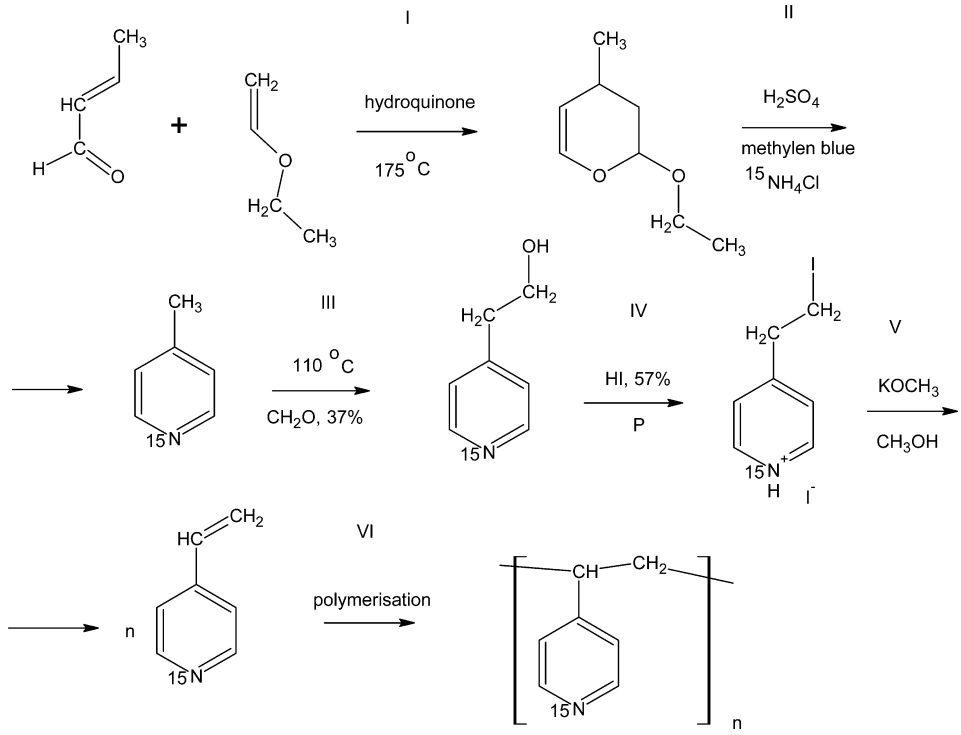

technique. The molar ratio of side chain units to free solvent molecules was 1:1. The gel samples were irradiated for 1.0−2.0 h using a calibrated xenon light source (L7810, Hamamatsu) at $\lambda = 385$ nm (fluorescence filter 386/23, BrightLine). Following irradiation, the samples were dried at room temperature in a vacuum chamber (10^{-3} atm, ShelLab) for 1.0−1.5 h, in order to reduce the concentration of free pyridine. Drying contributed to the stabilization of some of the photoinduced properties.

^{15}N labeled P4VPy was synthesized with a molecular weight of 200 000 (95% ^{15}N-enriched) (Scheme 1 and Supporting Information, Synthesis of ^{15}N 4-vinyl pyridine and poly(4-vinyl pyridine)). Gel samples were prepared with the labeled polymer and liquid pyridine as described above.

Photoinduced Emission. Photoluminescence spectra were measured on a Shimadzu RF-5301PC spectrofluorimeter with a resolution of 0.2 nm and with a xenon lamp light source, 5.1 mW/cm^2 at 385 nm. Emission lifetime measurements were made with a homemade device which included a frequency-tripled Nd:YAG laser, $\lambda = 355$ nm, a pulse duration of 5 ns (Continuum), and a photomultiplier tube PMT R 928 (Hamamatsu).

DFT modeling. We used the hybrid Hartree−Fock density functional theory (DFT) B3LYP (the Becke three-parameter Lee−Yang−Parr) method[16] as implemented in the Gaussian 03 program[17] in both its restricted (for singlet states) and unrestricted (for triplet states) forms in conjunction with Dunning's triple-ζ correlation consistent basis set (cc-pVTZ).[18] This allowed us to model the optimal structure, charge, and spin distributions of the pyridine side chain in the ground and excited states. The geometries of the molecules in the gas phase were fully optimized for all states without symmetry constraints, and local minima were characterized by frequency calculations (Supporting Information, Tables S1 and S2). Zero point vibrational energy (ZPE) corrections were taken into account in all calculations, and the results presented below include this correction.

Magnetic Susceptibility Measurements. The DC magnetic moment was measured at 125 K using a Quantum Design Co. SQUID MPMS XP field shielded magnetometer under both zero field cooled (ZFC) and field cooled (FC) conditions. Each measurement was repeated four times.

Electron Spin Resonance Spectroscopy. Experiments were performed with the Bruker ESR spectrometer ELEXSYS 500. The temperature was adjusted with a control unit (ER 4131VT) with an accuracy of ± 1 K. For g-factor calculations, the signal of DPPH ($g = 2.0037$) was used as a standard. The microwave power was 20 mW, and the modulation amplitude was 10^{-4} T.

Solid State ^{15}N-NMR Spectroscopy. CP NMR experiments were performed under MAS conditions with continuous proton decoupling. MAS spinning speeds were of the order of 5 kHz. The 90° pulse width was 4 μs, and the recycle time was 3 s. Variation of the CP contact times between 2 and 8 ms did not affect the spectra. All spectra were recorded on a Varian CMX 300 NMR spectrometer operating at 7 T and are referenced to external solid $^{15}NH_4Cl$ (95% ^{15}N-enriched).

Results

After two weeks of storage in the dark, the dry poly(4-vinyl pyridine) dissolved in dry liquid pyridine stabilized in the form of a homogeneous, amorphous gel, as shown by X-ray powder diffraction measurements.[15] The gel samples were irradiated for 1.0−2.0 h. Following irradiation, the samples were dried at room temperature in a vacuum chamber for 1.0−1.5 h, in order to reduce the concentration of liquid pyridine. The irradiated and vacuum-dried gel displays emission at 504 nm, the intensity of which increases with the time of irradiation at 385 nm (Figure 1A). The relatively long lifetime (~600 ns) measured at room temperature is evidence that the photoexcited electronic state is triplet rather than singlet in character (Figure 1B).

In order to gain insight into the possible location of the unpaired electronic spins, unrestricted B3LYP calculations were applied. To the best of our knowledge, the polymer forms a photosensitive system only in the presence of liquid pyridine.[19] The effect of the interaction of the parent molecule with the solvent was modeled by adding a free pyridine molecule to the

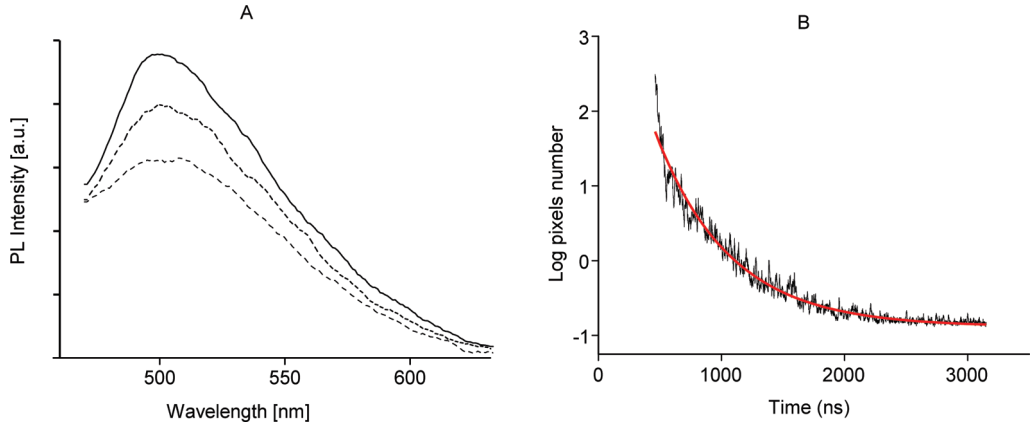

Figure 1. (A) Emission spectra of a thin layer (100 μm) of a P4VPy/Py gel irradiated at 385 $\pm$ 10 nm (xenon lamp, 5.1 mW/cm^2) for 0 min (dashed lines), 15 min (dotted lines), or 30 min (solid lines). Maximum emission is at 504 nm following excitation at 440 nm. (B) Decay of the emission at 504 nm following 1 h of irradiation and 1 h of evacuation (black curve); the red curve is the fit to monoexponential decay.

calculation. As can be seen below, the pyridine molecule serves as a vehicle for a proton transfer reaction similar to that described as class 4 by Kasha.[20] In the initial stage, the H_{11} atom is bound to the C_{11} atom and the free pyridine molecule is located near the pyridine side chain. The structure of the pyridine side chain in the presence of free pyridine and with a second pyridine side chain as the terminal group on the main chain was optimized on the singlet potential energy surface (Figure 2A, **1**). At the optimized singlet state geometry, the $H_{11}-N_2$ bond length is 3.417 Å and the singlet−triplet vertical excitation energy ΔE_{s-t}^{vert} is 398.74 kJ/mol (Figure 2B). Optimized model parameters are included in the Supporting Information.

Because the transfer of the H-atom (H_{11}) from C_{11} of the main chain to N_1 of the side chain pyridine is endothermic (−211.88 kJ/mol), such a transfer is not favorable on the singlet potential energy surface. Further optimization of **1** on the triplet potential energy surface (taking as a starting point the optimized geometry of the singlet state) leads to molecular structure **1a** (Figure 2A). Molecular structure **1a** is formed by hydrogen bonding of the protonated solvent pyridine to the nitrogen atom of the pyridine side chain. The reaction on the triplet potential energy surface is exothermic (about 205 kJ/mol), and therefore, such a proton transfer reaction is thermodynamically favorable. We emphasize that **1** is not a stationary point (local minimum) on the triplet potential energy surface. Our attempts to locate a local minimum in addition to **1a** or a transition state for the transformation from **1** to **1a** on the triplet potential energy surface were unsuccessful. We take that to mean that the structural change of **1** to **1a** (Figure 2B) occurs without a barrier. The electronic ground state of **1a** is a triplet (T_1) with a triplet−singlet vertical excitation energy of ΔE_{t-s}^{vert} =13.81 kJ/mol. To evaluate the influence, if any, of the adjacent side chain group on the photochemical reaction, we replaced the nearest neighbor side chain by a H-atom (see the Supporting Information). The results of the calculations for this molecule are similar to those obtained above (ΔE_{t-s}^{vert} = 21.34 kJ/mol). Therefore, we conclude that the nature of the terminal group R on the $C_{11}-CH_2-CH_2R$ chain has little influence on the properties of the molecules studied in both the singlet and triplet states.

The molecular conformation of **1a** is strongly polar with a dipole moment of 11.81 D in S_0 and 6.48 D in T_1. This indicates a potentially high sensitivity to an applied static electric field.[14] In the UB3LYP calculations of the triplet state, the spin contamination is very small ($\hat{S}^2$ is around 2.02) which means that the contribution of undesired spin states to the overall wave function is almost negligible and the UB3LYP method can be

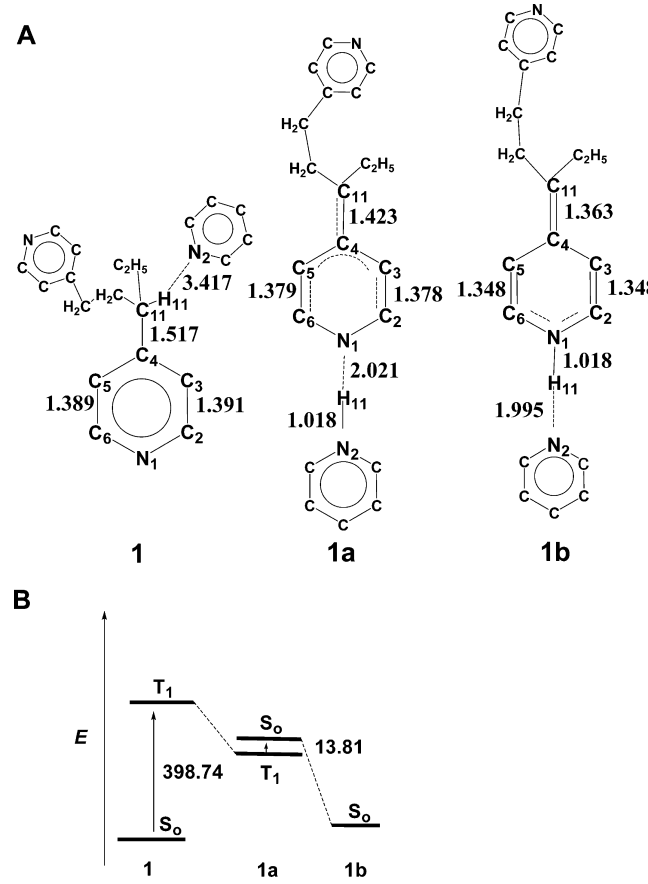

Figure 2. (A) Molecule **1** interacting with free pyridine following DFT optimization (molecular structure parameters listed in Tables S1 and S2 of the Supporting Information); bond lengths are in Å. (B) Energy level diagram for the three states of molecular structure **1** calculated using the B3LYP/cc-pVTZ method as implemented in the Gaussian 03 program. The placing of the energy levels on the vertical axis is not to scale. Energies are in kJ/mol.

safely applied to such a system. The Mulliken atomic charge and spin density distribution, calculated by the B3LYP/cc-pVTZ method, are presented in Table 1. We present values only for C_{11}, N_2, H_{11}, and the polymer non-hydrogen side chain atoms. Because molecule **1a** is in a triplet state, the total spin of the molecule is equal to 2. The values presented clearly show that the unpaired spin density in the triplet state of **1a** is primarily located on C_{11} (~0.7) and on the polymer pyridine ring (~0.65). The remainder of the unpaired spin density (~0.65) is delocal-

TABLE 1: Mulliken Atomic Charges (in Electrons) for Singlet and Triplet States of Molecules 1 and 1a and Mulliken Atomic Spin Density Distributions for the Triplet State of Molecule 1a Calculated Using the B3LYP/cc-pVTZ Method[a]

	singlet state		triplet state	
	charge distribution		charge distribution	spin distribution
atom	**1**	**1a**	**1a**	**1a**
N_1	−0.154	−0.269	−0.196	0.182
C_2	−0.100	−0.105	−0.083	−0.077
C_3	−0.079	−0.130	−0.104	0.194
C_4	−0.020	0.068	0.064	−0.114
C_5	−0.108	−0.123	−0.098	0.194
C_6	−0.095	−0.102	−0.080	−0.077
C_{11}	−0.062	−0.029	0.027	0.660
H_{11}	0.087	0.206	0.193	−0.008
N_2	−0.168	−0.015	−0.063	0.249

[a] Values are presented for C_{11}, N_2, H_{11}, and polymer side chain atoms only. The total charge of molecules **1** and **1a** (see Figure 2) equals 0; the total spin of molecule **1a** in the triplet equals 2.

ized over all other parts of the molecule (two pyridine rings, C_2H_5 and CH_2 groups) and is not presented in the table. The T_1 state of molecular structure **1a** may be long-lived, since it is in fact the ground state on the triplet potential energy surface. It is known that hydrogen bonding may increase the lifetime of a T_1 state,[21] and that more than one electronic state is usually involved in excited state proton transfer reactions.[21,22] On the other hand, due to the fact that the energy difference between the triplet and singlet energy surfaces for **1a** is relatively small (13.81 kJ/mol), spin inversion can occur and there is a probability for transferring the system on the singlet potential energy surface to the much more thermodynamically stable pyridinium polymer ion **1b**. In order for spin inversion (SI) to take place, the singlet and triplet potential energy surfaces should have a crossing point.[23] The minimum energy crossing point (MECP) was located with the B3LYP/cc-pVTZ level of DFT using the program developed by Harvey at al.[24] (Cartesian coordinates of the crossing point are given in Table S1 of the Supporting Information.) It lies just 1.59 kJ/mol above the triplet minimum of **1a** and 12.22 kJ/mol below the energy of **1a** on the singlet potential energy surface. It is possible to estimate the probability for a crossover at the spin inversion junction using the Landay−Zener treatment (see ref 23 for a discussion of this treatment). The probability is proportional to the spin orbit coupling matrix element between the two spin states, the effective velocity of passing through the crossing point, and the difference in the slopes of the two intersecting surfaces at the crossing point. Such calculations will be initiated in future work. The singlet state of **1b** is about 167.36 kJ/mol more stable than the triplet state of **1a** (Figure 2A, **1b**). In **1b**, the aromatic structure of the pyridine side chain has been converted to a conjugated structure of the quinoid type in its protonated form. While the initial, nonprotonated side chain is rotated by 60° with respect to the alkane chain, the protonated pyridine side chain is almost parallel to the direction of the alkane chain.

To search experimentally for evidence of the triplet state intermediate predicted by the DFT modeling, we first measured the magnetic susceptibility of the irradiated and evacuated gel as a function of both temperature and magnetic field. Typical results for the molar susceptibility measurements (formula weight = 105.139 g/mol) obtained at 4×10^4 and 1.2×10^5 Am^{-1} for both irradiated and nonirradiated samples are presented in Figure 3. The zero field cooled (ZFC) temperature dependence

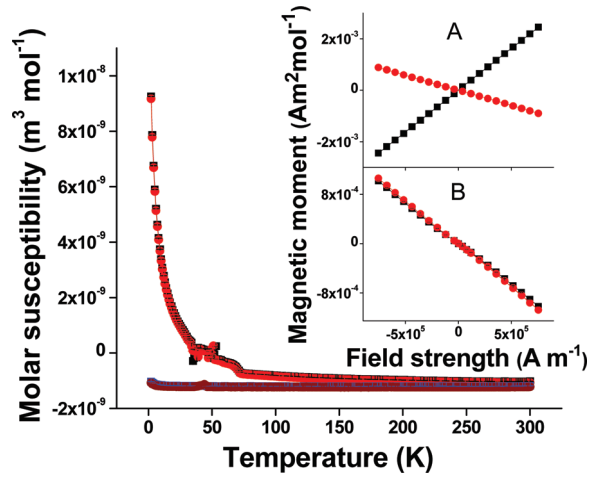

Figure 3. Temperature dependence of the molar magnetic susceptibility of a poly(4-vinyl pyridine)/pyridine gel sample: (black squares) following 2 h of irradiation at 385 nm (2.4 μW/cm^2 xenon lamp) and 1 h of evacuation, FC 4×10^4 Am^{-1}; (red circles) following irradiation and evacuation, FC 1.2×10^5 Am^{-1}; (red line) Curie law fit; (blue triangles) following 1 h of evacuation, FC 4×10^4 Am^{-1}; (maroon triangles) following evacuation, FC 1.2×10^5 Am^{-1}. Inset A: Field dependence of the magnetic moment of an irradiated, evacuated gel at 10 (black squares) and 300 K (red circles). Inset B: Field dependence of the magnetic moment of an evacuated gel at 10 (black squares) and 300 K (red circles).

of the susceptibility coincides with the field cooled (FC) dependence. Taking into account a temperature independent diamagnetic contribution to the susceptibility, $\chi_0 = -7.799(0) \times 10^{-9}$ m^3/kg, both curves can be satisfactorily described by Curie's law ($\chi = C/(T - \Theta)$), where C is the Curie constant and Θ is the Curie−Weiss temperature. Fitting with the Levenberg−Marquart procedure gives $C = 1.11(3) \times 10^{-6}$ emu*K/g and $\Theta = -4.04$ K. The nonirradiated samples demonstrated only temperature independent susceptibility (Figure 3) which comes from the orbital magnetism of the filled atomic electronic shells, and the bonding molecular orbitals together with the holder contribution. Increasing the time of irradiation increased the relative amount of the paramagnetic component: magnetic moments of 0.11 and 0.20 μ_B/mol for 1.0 and 2.0 h of irradiation, respectively. The paramagnetic properties are not permanent. After 10−15 h at 10 K, only the diamagnetic contribution to the susceptibility was observed. Material that had been irradiated but not vacuum-dried did not display paramagnetism. The fact that magnetic susceptibility measurements of the irradiated (2 h) gel gave a Curie constant corresponding to an effective magnetic moment of ∼0.2 μ_B/mol of irradiated material shows that, on average, an unpaired electron is present on one out of five vinyl pyridine monomers.

Paramagnetic behavior was also probed with electron spin resonance (ESR) measurements. The ESR signal at 125 K of a gel sample immediately following 1 h of irradiation and 1 h of vacuum drying is presented in Figure 4. The irradiated sample displays a prominent resonance with a g-factor of 2.199 and line width of 0.0199 T. A second weaker resonance was observed with a g-factor of 1.914 and aline width of 0.0050 T. g-factor calibration was based on DPPH ($g = 2.0037$). After 5 h in the dark at room temperature (Figure 4), the low field resonance is no longer observed. No low field resonance was observed for the gel sample which had undergone vacuum drying but not irradiation. Material that had been irradiated but not vacuum-dried also did not display a low field resonance. The high field resonance is identified (Figure 4) as being due

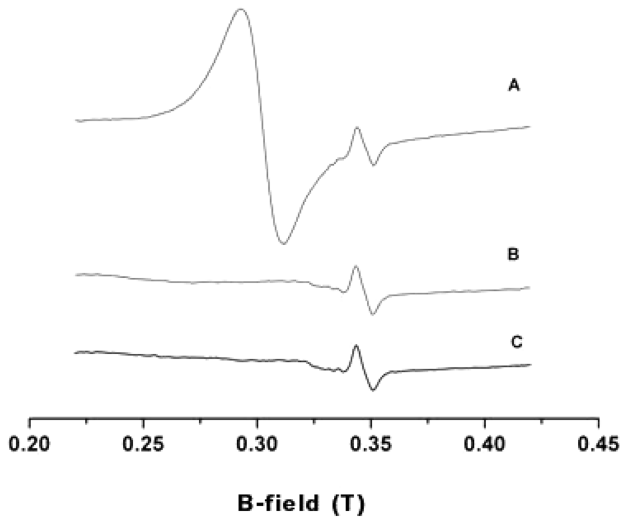

Figure 4. Low temperature (125 K) X-band ESR spectra of (A) poly(4-vinyl pyridine)/pyridine gel (weight 0.077 g) following 1 h of irradiation at 385 nm (2.4 μW/cm^2 xenon lamp) and 1 h under a vacuum (10^{-3} atm). (B) The same sample as for part A after 5 h at room temperature under Al foil. (C) The empty glass ESR tube. Experiments were performed with the Bruker ESR spectrometer ELEXSYS 500. The temperature was adjusted with a control unit (ER 4131VT) with an accuracy of $\pm$1 K. Microwave power 20 mW; modulation amplitude 10^{-4} T.

to magnetic impurities in the empty glass ESR tube. We identify the low field resonance as being due to uncompensated spins of the P4VPy/Py gel.

The low field resonance in Figure 4 is typical of a single unpaired spin, rather than a triplet species, and displays both a large line width and an unusually large value for the *g*-factor. At this point, we do not have an explanation for the latter even considering strong spin−orbit interactions. The large line width may have several causes. It may be accounted for by dipolar coupling of paramagnetic centers randomly oriented in a frozen matrix which produces inhomogeneous line broadening. However, when the gel is irradiated for 15 min instead of 1 h, with 1 h of vacuum drying, the same broad ESR signal is observed but with much lower intensity. This indicates that a high concentration of paramagnetic centers is not responsible for the large line width. Anisotropies of *g*-factors and/or hyperfine interactions are alternative causes. As far as the single spin character of the resonance is concerned, such behavior has indeed been observed previously for a long-lived, photoexcited triplet biradical intermediate when one of the unpaired electrons is well localized and the second is significantly delocalized.[25] As described above, the DFT modeling predicts such a distribution of unpaired electrons for the P4VPy/Py system studied here. We also note that the time scale probed by the measurement may be responsible for some of the ESR features described here.

A solid sample of $CuSO_4 \cdot 5H_2O$ of known weight was used as a standard for estimation of the concentration of paramagnetic centers by double integration of the ESR signal. The result is $\sim 7 \times 10^{18}$ electrons/g with an accuracy of $\pm$20%.

The presence of the more thermodynamically stable protonated pyridine side chains, as predicted by DFT modeling (molecule **1b**, Figure 2), was detected at room temperature in the irradiated 95% ^{15}N-enriched P4VPy/Py gel. The room temperature CP MAS solid state ^{15}N NMR spectra were measured both before and after 1 h of irradiation at 385 nm (Figure 5). Prior to irradiation, one peak due to the chain pyridine is observed at 270 ppm. The chemical shift is similar

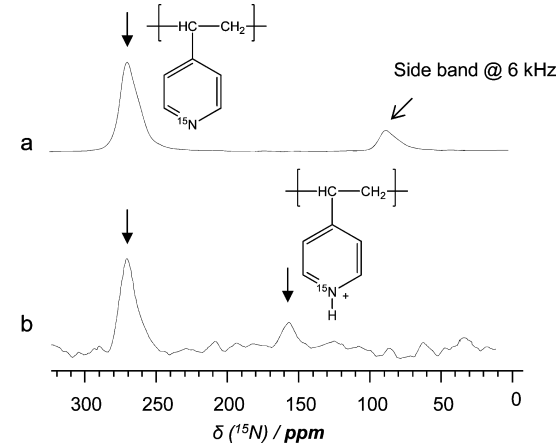

Figure 5. Room temperature ^{15}N CP MAS NMR spectra of (a) gel prepared with ^{15}N labeled P4VPy and nonlabeled bulk pyridine without irradiation and (b) gel prepared with ^{15}N labeled P4VPy and nonlabeled bulk pyridine after 2 h of irradiation at 385 nm and 10 min of measuring time. M_w of the polymer: 200 000 Da. The variation of the CP contact times between 2 and 8 ms did not affect the spectra. All spectra are referenced to external solid $^{15}NH_4Cl$ (95% ^{15}N-enriched). (The arrows denote the resonance peaks.)

to those obtained for neat frozen pyridine and collidine, 278 and 268 ppm, respectively.[26] Irradiation gave rise to an additional weak signal, high field shifted with respect to the first by 115 ppm. Such a shift is characteristic of protonated pyridines such as the pyridinium cation, 172 ppm, and the collidinium cation, 148 ppm.[24] The protonation is reversible. The intensity of the signal attributed to the protonated pyridine side chains decreases with time and disappeared after 1 h. It is known that hydrogen bonding may increase the lifetime of a tautomer state.[21]

Conclusion

We have presented experimental evidence in support of a possible mechanism for photoexcited proton transfer in a poly(4-vinyl pyridine)/pyridine gel. According to DFT modeling, following irradiation at 385 nm, the proton donor is the CH group of the polymer main chain and the proton acceptor is the nitrogen of the polymeric pyridine side chain. Proton transfer is made possible through the assistance of the mobile pyridine solvent molecule acting as a transfer vehicle. This process may be relevant for photosensitive devices as well as being considered as a possible model for photochemical processes in biological systems. Nevertheless, in order to prove that the different chemical species of the multistep photochemical reaction are related via specific chemical processes, it will be necessary to determine minimum energy paths as well as the magnitude of the spin orbit coupling. We do plan to undertake this type of calculation at a later date. On the basis of our experimental results, we also conclude that long-lived paramagnetism may be included among the inducible properties of soft polymer gels.

Acknowledgment. We thank Dr. Lev Weiner of the Weizmann Institute of Science for the ESR measurements and Prof. Uri Banin and Ph.D. student Amit Sitt of the Hebrew University of Jerusalem for the luminescence lifetime measurements. E.V. gratefully acknowledges financial support from the Israel Ministry for Immigrant Absorption. This work was supported in part by the EC through contract FP6-029192 (E.V. and S.Y.).

Supporting Information Available: The Materials and Methods section and supporting figures and tables. This

information is available free of charge via the Internet at http://pubs.acs.org.

References and Notes

(1) De Gennes, P. G. *Macromolecules* **1976**, *9*, 587–598.
(2) Johlin, J. M. *Science* **1932**, *75*, 462.
(3) Tanaka, T.; Nishio, I.; Sun, S.-T.; Ueno-Nishio, S. *Science* **1982**, *218*, 467–469.
(4) Tokita, M.; Tanaka, T. *Science* **1982**, *253*, 1121–1123.
(5) Hu, Z.; Zhang, X.; Li, Y. *Science* **1995**, *269*, 525–527.
(6) Yashin, V. V.; Balazs, A. C. *Science* **2006**, *314*, 798–801.
(7) Siegel, R. A.; Firestone, B A. *Macromolecules* **1998**, *21*, 3254–3259.
(8) Mamada, A.; Tanaka, T.; Kungwatchakun, D.; Irie, D. *Macromolecules* **1990**, *23*, 1517–1519.
(9) Suzuki, A.; Tanaka, T. *Nature* **1990**, *346*, 345–347.
(10) Juodkazis, S.; et al. *Nature* **2000**, *408*, 178.
(11) Li, Y.; Sun, Z.; Su, Z.; Shi, T.; An, L *J. Chem. Phys.* **2005**, *122*, 194909-1–194909-6.
(12) Burlatsky, S.; Deutch, J. *Science* **1993**, *260*, 1782–1784.
(13) Wan, W.; Whittenburg, S. L. *Macromolecules* **1986**, *19*, 925–927.
(14) Berestetsky, N.; et al. *J. Phys. Chem. B* **2008**, *112*, 3662–3667.
(15) Vaganova, E.; Meshulam, G.; Kotler, Z.; Rozenberg, M; Yitzchaik, S. *J. Fluoresc.* **2000**, *10*, 81–88.
(16) Kohn, W.; Holthausen, M. C. *A Chemist's Guide to Density Functional Theory*; Wiley-VCH: New York, 2001.
(17) Frisch, M. J. *Gaussian 03*, revision C.02; Gaussian, Inc.: Wallingford, CT, 2004.
(18) Dunning, T. H., Jr. *J. Chem. Phys.* **1989**, *90*, 1007–1023.
(19) Vaganova, E.; Yitschaik, S. *Acta Polym.* **1998**, *49*, 636–641.
(20) Kasha, M. *J. Chem. Soc., Faraday Trans. 2* **1986**, *82*, 2379–2392.
(21) Eichen, Y.; et al. *J. Chem. Soc., Chem. Commun.* **1995**, 713–714.
(22) Godfrey, T. S.; Porter, G.; Suppan, P. *Discuss. Faraday Soc.* **1965**, *39*, 194–199.
(23) Danovich, D.; Shaik, S. *J. Am. Chem. Soc.* **1997**, *119*, 1773–1786.
(24) Harvey, J. N.; Aschi, M.; Schwarz, H.; Koch, W. *Theor. Chem. Acc.* **1998**, *99*, 95–99.
(25) Sajimon, M. C.; Ramaiah, D.; Suresh, C. H.; Adam, W.; Lewis, F. D.; George, M. V. *J. Am. Chem. Soc.* **2007**, *129*, 9439–9445.
(26) Lorente, P.; et al. *Magn. Reson. Chem.* **2001**, *39*, S18–S29.

JP104277R